


Carnosine Inhibits the Proliferation of Human Cervical Gland Carcinoma Cells Through Inhibiting Both Mitochondrial Bioenergetics and Glycolysis Pathways and Retarding Cell Cycle Progression

Integrative Cancer Therapies
2018, Vol. 17(1) 80–91
© The Author(s) 2016
Reprints and permissions:
sagepub.com/journalsPermissions.nav
DOI: 10.1177/1534735416684551
journals.sagepub.com/home/ict


Yun Bao, MS^{1,2}, Saidan Ding, PhD³, Jiaoyan Cheng, BS¹, Yuan Liu, BS¹, Bingyu Wang, BS¹, Huijuan Xu, BS¹, Yao Shen, PhD¹, and Jianxin Lyu, PhD¹

Abstract

Carnosine has been demonstrated to play an antitumorigenic role in certain types of cancer. However, its underlying mechanism is unclear. In this study, the roles of carnosine in cell proliferation and its underlying mechanism were investigated in the cultured human cervical gland carcinoma cells HeLa and cervical squamous carcinoma cells SiHa. The results showed that carnosine exerted a significant inhibitory effect on the proliferation of HeLa cells, whereas its inhibitory action on the proliferation of SiHa cells was much weaker. Carnosine decreased the ATP content through inhibiting both mitochondrial respiration and glycolysis pathways in cultured HeLa cells but not SiHa cells. Carnosine reduced the activities of isocitrate dehydrogenase and malate dehydrogenase in TCA (tricarboxylic acid) cycle and the activities of mitochondrial electron transport chain complex I, II, III, and IV in HeLa cells but not SiHa cells. Carnosine also decreased the mRNA and protein expression levels of ClpP, which plays a key role in maintaining the mitochondrial function in HeLa cells. In addition, carnosine induced G1 arrest by inhibiting the G1-S phase transition in both HeLa and SiHa cells. Taken together, these findings suggest that carnosine has a strong inhibitory action on the proliferation of human cervical gland carcinoma cells rather than cervical squamous carcinoma cells. Mitochondrial bioenergetics and glycolysis pathways and cell cycle may be involved in the carnosine action on the cell proliferation in cultured human cervical gland carcinoma cells HeLa.

Keywords

carnosine, cell cycle, human cervical cancer cells, isocitrate dehydrogenase, malate dehydrogenase, mitochondrial bioenergetics, mitochondrial electron transport chain (ETC)

Submitted June 1, 2016; revised November 6, 2016; accepted November 11, 2016

Introduction

Cervical cancer is the third most common malignancy in women worldwide. Human papillomavirus (HPV) infection is the most frequent risk factor in the development of nearly all cases of cervical cancer.^{1,2} In early stage, cervical cancer is potentially curable through a combination of surgery, radiation therapy, or chemotherapy. The 5-year survival rate exceeds 90%. The routine use of Pap smear and HPV tests has significantly improved the outcome of cervical cancer in developed countries.³ Unfortunately, patients in lower income countries are often diagnosed at an advanced stage because of the lack of adequate screening, early diagnosis, and curative treatments.⁴ Despite the

fact that most molecular research efforts have been based on the link between high-risk HPV types and cervical

¹Wenzhou Medical University, Wenzhou, Zhejiang, Peoples Republic of China

²Jinhua People's Hospital, Jinhua, Zhejiang, Peoples Republic of China

³The First Affiliated Hospital of Wenzhou Medical University, Wenzhou, Zhejiang, Peoples Republic of China

Corresponding Author:

Yao Shen, Key Laboratory of Laboratory Medicine, Ministry of Education, Attardi Institute of Mitochondrial Biomedicine, College of Laboratory Medicine and Life sciences, Wenzhou Medical University, Wenzhou, Zhejiang 325035, Peoples Republic of China.

Email: yueshen-2002@163.com



Creative Commons Non Commercial CC-BY-NC: This article is distributed under the terms of the Creative Commons

Attribution-NonCommercial 3.0 License (<http://www.creativecommons.org/licenses/by-nc/3.0/>) which permits non-commercial use, reproduction and distribution of the work without further permission provided the original work is attributed as specified on the SAGE and Open Access pages (<https://us.sagepub.com/en-us/nam/open-access-at-sage>).

cancer, the identification of novel molecular targets and mechanisms contributing to improved treatment for this disease will be meaningful.

Carnosine (β -alanyl-L-histidine), a naturally occurring dipeptide consisting of β -alanine and L-histidine, is synthesized by carnosine synthetase. As an endogenous substance, it is highly concentrated in muscle and brain tissues and also presents in other organs such as lungs, kidney, and stomach.⁵ Since the discovery of carnosine, repeated clinical efforts have been consistently made to determine its biological functions, and several physiological functions have been pointed out, including antioxidant activity, neurotransmitter function, anti-inflammatory, and anti-senescence properties.⁵⁻⁹ So it is not surprising that the enigmatic peptide is increasingly found to be implicated in an increasing number of pathological conditions. For example, it is found to be related to tumors. It has been reported that carnosine regulated some events that contribute to the tumor growth and metabolism, highlighting the critical importance of carnosine's antitumorigenic effect.¹⁰⁻¹³ Although it has been suggested that carnosine is involved in cell proliferation, cell cycle arrest, cell apoptosis, and even the glycolytic energy metabolism of certain tumor cells, the molecular mechanisms of the antineoplastic activities of this dipeptide are still not completely understood.¹⁴

Recently, the importance of mitochondria as oxygen sensors as well as producers of ATP has become a focal point of cancer research, and studies have showed an important phenomenon that mitochondrial metabolism is important for the rapid proliferation of multiple cancer cell types.^{15,16} Therefore, the current study was designed to explore whether carnosine could inhibit the proliferation of human cervical cancer cells, and whether the mitochondrial bioenergetics or the glycolysis pathway and/or any other mechanisms contribute to the carnosine action on the proliferation of human cervical cancer cells.

Materials and Methods

Reagents

L-Carnosine, rotenone, carbonyl cyanide p-trifluoromethoxyphenyl-hydrazone (FCCP), and Oligomycin were from Sigma (St Louis, MO). Dulbecco's modified Eagle's medium (DMEM) was from Hyclone (USA). Fetal bovine serum (FBS) was from NATOCOR (Argentina). Annexin V-FITC/PI apoptosis detection kit was from Lianke Biotechnology Co, Ltd. 3-[4,5-Dimethylthiazol-2-yl]-2,5-diphenyltetra-zolium bromide (MTT), BCA protein assay kit, and ATP assay kit were from Beyotime Institute of Biotechnology (Nanjing, China). XF assay medium and XF calibrant solution were obtained from Seahorse Bioscience (USA). RNA Extraction Kit, PrimeScript RT reagent kit, and SYBR Premix Ex Taq were from TakaRa Biotechnology

(Dalian) Co, Ltd (Dalian, China). Cell cycle detection kit and lactic acid assay kit were from Jiancheng Bioengineering Institute (Nanjing, China).

Cell Culture and Carnosine Treatment

The human cervical gland carcinoma cells HeLa and cervical squamous carcinoma cells SiHa were purchased from American Type Culture Collection (Rockville, MD). Cells were cultured in DMEM supplemented with 10% FBS and antibiotics (100 U/mL penicillin G and 100 μ g/mL streptomycin) at 37°C in a humidified atmosphere of 5% CO₂. One mole of stock solution of carnosine was made in phosphate-buffered saline (PBS) immediately before use, and cells were treated with carnosine at a final concentration of 20 mM for 48 hours.

Colony Formation Assay

Cells were plated in 6-well plates at density of 200 to 300 cells per well and then were treated with carnosine (20 mM). Clones were allowed to grow for 14 days in DMEM culture medium supplemented with 10% FBS, 100 U/mL penicillin G, and 100 μ g/mL streptomycin, and the medium was changed every 3 to 4 days. The cells were subsequently fixed with 4% paraformaldehyde and stained with crystal violet for analysis of colony formation.¹⁷

MTT Reduction Assay

Cell metabolic activity was monitored by the colorimetric MTT assay as described previously.¹⁸ Briefly, cells were cultured on 96-well plates and there were 10 wells in each group. At the end of experiments, the cells were incubated with 0.5 mg/mL MTT for 4 hours at 37°C. Then, the supernatant layer was removed, and 100 μ L of dimethyl sulfoxide was added into each well. MTT metabolism was quantitated spectrophotometrically at 570 nm in a BioRad microplate reader. Results were expressed as the percentage of MTT reduction, taking the absorbance of control cells as 100%.

Cell Apoptosis Analysis

The percentage of apoptotic cells was measured using an Annexin V-FITC apoptosis detection kit according to the manufacturer's protocol. The HeLa and SiHa cells were treated with carnosine (20 mM) for 48 hours, and then were harvested and washed twice with PBS. The cells were resuspended in 500 μ L binding buffer containing 5 μ L Annexin V-FITC and 10 μ L PI. Then the cells were incubated away from light for 10 to 15 minutes at room temperature. Last, the stained cells were analyzed using a flow cytometer.

Seahorse XF96 Flux Analyzer

The Seahorse XF96 Flux Analyzer (Seahorse Bioscience, Billerica, MA) was used to determine the metabolic profiles of HeLa and SiHa cells under the influence of carnosine. A total of 1.0×10^5 cells/well were seeded into XF96 microplates and incubated at 37°C for 24 hours. Thereafter, the cells were treated for 48 hours with 20 mM carnosine. After treatment, the cells were switched to unbuffered DMEM supplemented with 2 mM sodium pyruvate and 20 mM carnosine 1 hour prior to the beginning of the assay and maintained at 37°C. After baseline measurements, oxygen consumption rates (OCRs) and extracellular acidification rates (ECARs) were measured after sequentially adding to each well 20 μ L of oligomycin (which blocks the mitochondrial complex V, where the electron chain is coupled to ATP synthesis), FCCP (an uncoupling agent that allows maximum electron transport), and rotenone (which blocks complex I, thereby eliminating mitochondrial respiration), to reach working concentrations of 1 μ g/mL, 1 μ M, and 1 μ M, respectively. Each parameter, including ATP-linked OCR, proton leak, mitochondrial respiration OCR, and non-mitochondrial respiration OCR, is derived as described previously.¹⁹ OCR is reported in the unit of picomoles per minute, and ECAR is reported in milli-pH units (mpH) per minute.

Extracellular Lactic Acid Level Assay

After carnosine treatment, the concentration of lactic acid in the cell-free supernatant was measured by the lactic acid assay kit according to the manufacturer's instruction.

Determination of ATP Production

The ATP assay was performed according to the manufacturer's instruction. Briefly, after carnosine treatment, the cells were harvested and lysed with a lysis buffer, followed by centrifugation at $10\,000 \times g$ for 2 minutes at 4°C. Finally, in 96-well plates, the level of ATP was determined by mixing 20 μ L of the supernatant with 100 μ L of luciferase reagent, which catalyzed the light production from ATP and luciferin. Luminance was measured by a monochromator microplate reader. Standard curves were also generated and the protein concentration of each treatment group was determined using the BCA protein assay kit. Total ATP levels were expressed as nmol/mg protein.

Western Blot Analysis

The cells were treated with carnosine for 48 hours and then were lysed in Western and IP lysis buffer containing PMSF for 5 minutes on ice, followed by centrifugation at $13\,000 \times g$ for 25 minutes at 4°C. The supernatant was harvested, and the protein concentration was quantified using a BCA

protein assay kit. Western blot analysis was carried out by standard protocol. The following antibodies were used: rabbit anti-c-Myc antibody (1:5000, ab32072), rabbit anti-PCNA antibody (1:1000, ab92552), rabbit anti-Bcl-2 antibody (1:1000, ab32124), rabbit anti-SDHA antibody (1:1000, ab137040), rabbit anti-IDH3A antibody (1:1000, ab58641), rabbit anti-MDH1 antibody (1:1000, ab180152), rabbit anti-ClpP antibody (1:1000, ab124822), rabbit anti-ClpX antibody (1:1000, ab168338), rabbit anti-COX IV antibody (1:1000, ab66739) (from Abcam Inc). Mouse anti- β -actin antibody (1:1000, AA128), HRP-labeled goat anti-rabbit IgG (1:500, A0208), and HRP-labeled goat anti-mouse IgG (1:500, A0216) were from Beyotime Institute of Biotechnology (Nanjing, China).

Isolation and Purification of Mitochondria

Mitochondria purification was conducted as described previously.²⁰ In brief, the cells were collected and homogenized in precooled homogenization buffer (0.25 M sucrose, 10 mM HEPES-NaOH, pH 7.4, 1 mM EDTA). Crude mitochondria were enriched by differential centrifugation and were further purified by centrifugation in a 30% to 55% sucrose density gradient at $135\,000 \times g$ for 15 minutes. Mitochondria fraction was collected at the interface of 40%/55% density and resuspended in mitochondria extraction buffer. An additional centrifugation at $12\,000 \times g$ for 30 minutes was carried out to get the final purified mitochondria pellet.

Dehydrogenase Activity Assay

α -Ketoglutarate dehydrogenase (α -KGD) activity was assayed by measuring the reduction of NAD^+ at 340 nm on the addition of 0.5 mM NAD^+ , 200 μ M TPP, 130 μ M CoA, and 2 mM α -KGD to 2 μ g/ μ L mitochondria. Isocitrate dehydrogenase 3 (IDH3) activity was assayed by measuring the reduction of NAD^+ at 340 nm on the addition of 167 μ M NAD^+ and 167 μ M (+)-potassium Ds-threoisocitrate monobasic to 2 μ g/ μ L mitochondria. Malate dehydrogenase (MDH) activity was assayed by measuring the reduction of NAD^+ at 340 nm on the addition of 0.5 mM NAD^+ and 5 mM malate to 2 μ g/ μ L mitochondria.^{21,22} Enzyme activity in the sample was calculated using an NADH extinction coefficient of 6.2 mM/cm.

Mitochondrial Electron Transport Chain (ETC) Complexes Activity Assays

Mitochondrial respiratory chain enzymatic activities (complexes I-IV) were assessed as previously described.¹⁷

Complex I activity: Prepared mitochondria (2 μ L; 2 μ g/ μ L) were added to the assay medium containing potassium phosphate buffer (10 μ L; 0.5 M; pH 7.5), fatty

acid-free BSA (12 μL ; 25 mg/mL), NaN_3 (1 μL ; 0.5 M), NADH (1 μL , 10 mM), and distilled water (73 μL). After reading the baseline at 340 nm for 2 minutes, ubiquinone₁ (1 μL ; 5 mM) was applied and the decrease in absorbance was recorded at 340 nm for 2 minutes. In parallel, the same quantity of reagents and samples but with the addition of rotenone solution (1 μL ; 1 mM) was used.

Complex II activity: Prepared mitochondria (2 μL ; 2 $\mu\text{g}/\mu\text{L}$) were added to the assay medium containing potassium phosphate buffer (5 μL ; 0.5 M; pH 7.5), fatty acid-free BSA (4 μL ; 25 mg/mL), NaN_3 (1 μL ; 0.5 M), succinate (5 μL ; 400 mM), DCPIP (14.5 μL ; 0.015% [wt/vol]), and distilled water (67.5 μL). The mixture was incubated at 37°C for 8 minutes, and then the baseline was recorded at 600 nm for 2 minutes. Then DUB (1 μL ; 5 mM) was applied and the decrease in absorbance at 600 nm was recorded for 2 minutes. In parallel, malonate (1 μL ; 1 M) was used.

Complex III activity: Prepared mitochondria (2 μL ; 2 $\mu\text{g}/\mu\text{L}$) were added to the assay medium containing potassium phosphate buffer (5 μL ; 0.5 M; pH 7.5), oxidized cytochrome c (7.5 μL ; 1 mM), NaN_3 (1.5 μL ; 0.5 M), EDTA (2 μL ; 5 mM; pH 7.5), Tween-20 (1 μL ; 2.5% [vol/vol]), and distilled water (80 μL). After reading the baseline at 550 nm for 2 minutes, decylubiquinol (1 μL ; 5 mM) was used and then the increase in absorbance at 550 nm was recorded for 2 minutes. In parallel, the same quantity of reagents and samples with the addition of antimycin A (1 μL ; 1 mg/mL) were used.

Complex IV activity: Reduced cytochrome c (5 μL ; 1 mM) was added to the potassium phosphate buffer (25 μL ; 100 mM; pH 7.0) and distilled water (40 μL). The baseline activity was recorded at 550 nm for 2 minutes. Then the prepared mitochondria (2 μL ; 2 $\mu\text{g}/\mu\text{L}$) were added to the assay medium, and the decrease in absorbance at 550 nm was recorded for 2 minutes. The specificity of complex IV activity was checked in parallel experiment, in which NaN_3 (1 μL ; 0.5 M) was added. The enzymatic activities for each mitochondrial enzyme should be calculated according to the following equation:

$$\text{Enzyme activity (nmol min}^{-1}\text{mg}^{-1}) = (\Delta\text{Dabsorbance} / \text{min} \times 1000) / [(\text{extinction coefficient} \times \text{volume of sample used in mL}) \times (\text{sample protein concentration in mg mL}^{-1})]$$

Quantitative Real-Time Polymerase Chain Reaction (PCR)

Total RNA was isolated with Trizol reagent according to the manufacturer's guidelines and was quantified by Nanodrop spectrophotometry. cDNA was synthesized from 2000 ng

total RNA using the PrimeScript RT reagent kit according to the manufacturer's instructions. Real-time quantification PCRs of ClpP, pepT1, and pepT2 were performed using SYBR Premix Ex Taq. All expression values of target genes were calculated using the $2^{-\Delta\Delta\text{Ct}}$ method.^{23,24} The primers used for the experiment were as follows: ClpP (Fw: 5'-ctcattccatcgtgggtgga-3'; Rev: 5'-gataacaaggctggcaacgc-3'), hpepT1 (FW: 5'-caatctgattctgtacttcac-3'; Rev: 5'-acatggcttgaacttcc-3'), hpepT2 (FW: 5'-tcacttcacctgaaatcac-3'; Rev: 5'-ctgtatcctttaccatcatgct-3'), β -actin (Fw: 5'-ggctgattccctecatcg-3'; Rev: 5'-ccagttggaacaatgccatgt-3').

Detection of the Cell Cycle Stage

The cell cycle of cervical cancer cells was measured by a cell cycle detection kit. The HeLa and SiHa cells were plated in 6-well plates and were maintained in fresh culture medium overnight, and were then treated with carnosine (20 mM) for 48 hours in the following day. The cervical cancer cells were collected after carnosine treatment and washed twice with PBS. Then, the cells were punched by 10 μL permeabilization solution and labeled with 1 mL DNA staining solution for 30 minutes. The fractions of the cells in G1, S, and G2 phases were analyzed by flow cytometry.

Statistical Analysis

All data represent 3 or more independent experiments. Data were expressed as mean \pm SD. Statistical analyses were conducted by SPSS 11.5 for Windows. One-way ANOVA (analysis of variance) followed by LSD (least significant difference) or Dunnett's T3 post hoc test (where equal variances were not assumed) was applied for multiple comparisons, whereas Student's *t* test was used for comparisons between 2 groups. $P < .05$ was considered statistically significant.

Results

Effect of Carnosine on HeLa and SiHa Cells Viability

To determine the effect of carnosine on HeLa and SiHa cells viability, MTT reduction assay was used. As shown in Figure 1A, carnosine at concentrations of 5, 20, and 50 mM markedly reduced cell viability to 88.09%, 67.82%, and 21.89% of control in HeLa cells and to 97.59%, 81.58%, and 65.32% of control in SiHa cells, respectively. Carnosine at a concentration of 100 mM caused massive cell death both in HeLa and SiHa cells as most of the cells were floated in the culture medium (data not shown). Therefore, carnosine at a concentration of 20 mM was used in the following tests. We further used flow cytometry to assay whether carnosine could also cause apoptosis in cultured HeLa and SiHa cells. The results showed that 20 mM carnosine

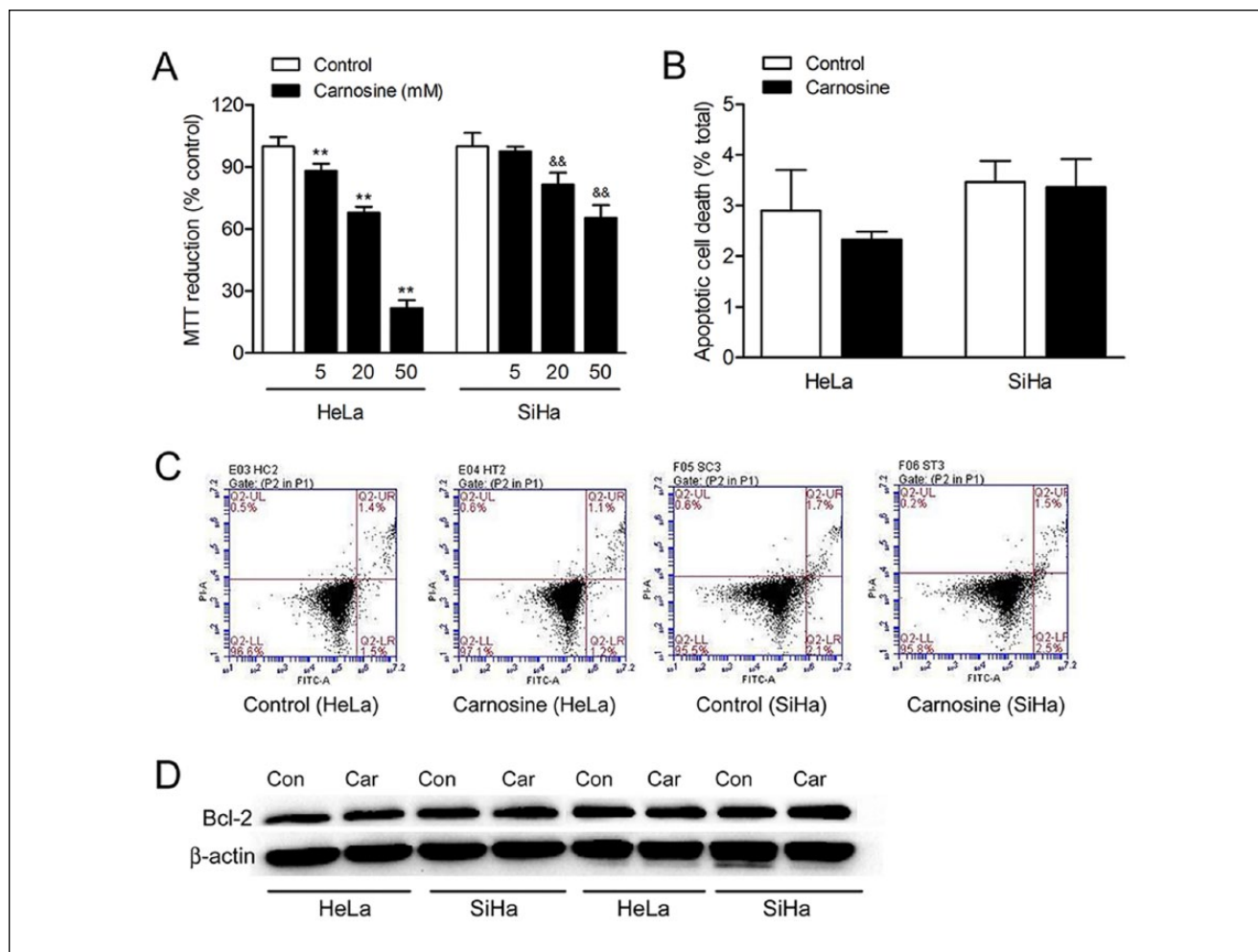


Figure 1. Effect of carnosine on cell viability in cultured HeLa and SiHa cells. Cells were treated with 5, 20, and 50 mM carnosine for 48 hours, respectively, and then the cell viability was assayed using the MTT reduction assay (A). Results were expressed as percentage of control, and were showed as mean \pm SD. N = 10-12. ** $P < .01$ versus control group in cultured HeLa cells, && $P < .01$ versus control group in cultured SiHa cells. Apoptotic cell death was determined by PI and Annexin V-FITC staining followed by flow cytometry (B, C). Western blot analysis of the expression of Bcl-2 in HeLa and SiHa cells after carnosine treatment for 48 hours (D).

treatment for 48 hours did not induce apoptotic cell death in HeLa or SiHa cells (Figure 1B, C). Moreover, we also found that carnosine treatment did not affect the expression level of Bcl-2 (Figure 1D).

Chronic Treatment With Carnosine Inhibited HeLa Cells Colonies Formation

To examine whether chronic exposure to carnosine could affect the proliferative capacity of HeLa and SiHa cells, the cells were seeded at a low density (200-300 cells/well) and allowed to form colonies for 14 days in DMEM supplemented with 20 mM carnosine. As shown in Figure 2, chronic exposure to carnosine resulted in a significant reduction in colonies formation in HeLa cells (control group: $100.00 \pm 5.42\%$, carnosine-treated group: $38.74 \pm 5.29\%$,

$P < .01$) and a slight reduction in colonies formation without statistical significance in SiHa cells (control group: $100.00 \pm 7.98\%$, carnosine-treated group: $86.97 \pm 8.66\%$, $P = .128$).

Carnosine Modulated Mitochondrial Bioenergetics and Glycolysis of Cultured HeLa Cells

We investigated the effects of carnosine on the oxygen consumption rate and extracellular acidification rate in cultured HeLa and SiHa cells. As shown in Figure 3, after treatment with 20 mM carnosine for 48 hours, the basal cellular OCR was found to be 239.5 ± 21.6 pmol/min/mg protein ($\sim 83.7\%$ of control) in HeLa cells and 436.1 ± 49.4 pmol/min/mg protein ($\sim 83.3\%$ of control) in SiHa cells (Figure 3A, C). Carnosine treatment also markedly reduced the basal cellular ECAR both in HeLa and SiHa cells (Figure 3B). Carnosine

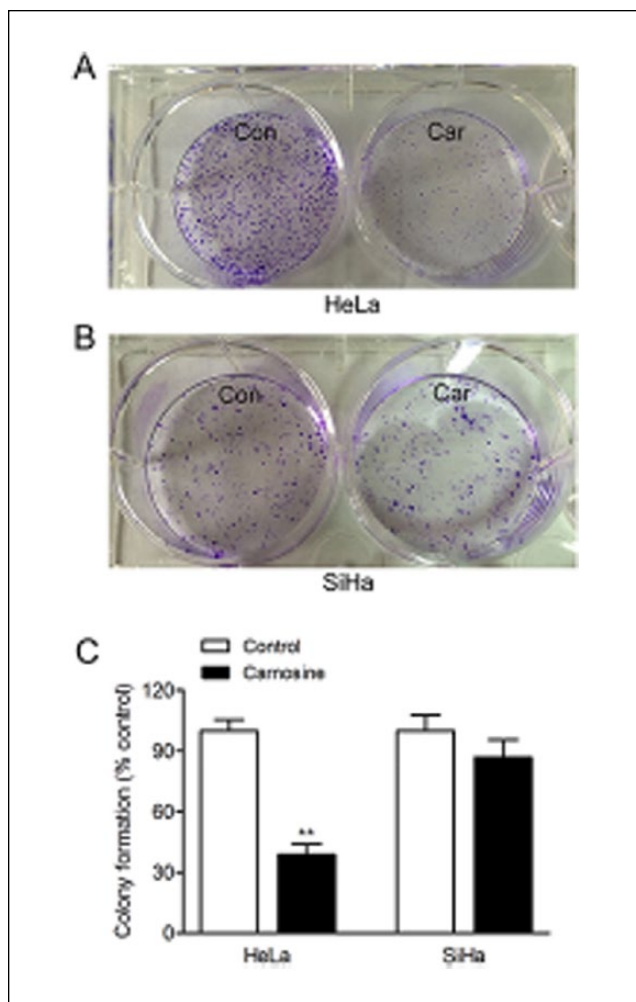


Figure 2. Effect of carnosine on colony formation in cultured HeLa and SiHa cells. Cells were seeded at low density in DMEM supplement with or without carnosine (20 mM) for 14 days. The colonies were subsequently fixed with 4% paraformaldehyde and stained with crystal violet for analysis of colony formation. Representative images of the cloning wells, HeLa cells (A), SiHa cells (B). Quantitative image analysis of colonies in cultured HeLa and SiHa cells (C). Data were expressed as mean \pm SD. N = 6. ** $P < .01$ versus control group.

markedly reduced the absolute amount of ATP-linked respiration and mitochondrial oxygen consumption rates in HeLa cells (Figure 3D, F), but it reduced non-mitochondrial oxygen consumption rates in SiHa cells (Figure 3G).

Carnosine is a mobile organic pH buffer. So the extracellular acidification rate assayed in the presence of carnosine cannot reflect the real glycolysis rate. So we also measured the extracellular lactic acid level to verify the effect of carnosine on glycolysis in cultured HeLa and SiHa cells. The results showed that carnosine treatment markedly reduced the extracellular lactic acid level to 69% of control in HeLa cells, whereas it did not affect the extracellular lactic acid level in SiHa cells (Figure 3H). Carnosine treatment also

significantly reduced the cellular ATP production in HeLa cells but not in SiHa cells (Figure 3I).

Carnosine Reduced the Activities of IDH3 and MDH in Cultured HeLa Cells

We next examined the enzymes activation of α -KGD, IDH, and MDH in tricarboxylic acid (TCA) cycle under the influence of carnosine. We found that carnosine treatment did not affect the activity of α -KGD, whereas the activities of IDH3 and MDH were significantly decreased after carnosine treatment (Figure 4A-C). The western blot analysis showed that carnosine treatment did not affect α -KGD, succinate dehydrogenase complex, subunit A (SDHA), IDH3, and MDH proteins expression level in cultured HeLa and SiHa cells (Figure 4D).

Carnosine Decreased the Activities of Mitochondrial Electron Transport Chain (ETC) in Cultured HeLa Cells

We also determined whether carnosine can also affect the activities of ETC complex I, II, III, and IV in cultured HeLa and SiHa cells. The results showed that carnosine treatment did not affect the activities of complexes I to IV in SiHa cells. However, it markedly reduced the activities of complexes I to IV in HeLa cells (Complex I, control group: 100.00 \pm 4.03%, carnosine-treated group: 86.85 \pm 2.50%, $P = .009$; Complex II, control group: 100.00 \pm 5.84%, carnosine-treated group: 76.44 \pm 3.83%, $P = .004$; Complex III, control group: 100.00 \pm 6.69%, carnosine-treated group: 80.06 \pm 5.21%, $P = .015$; Complex IV, control group: 100.00 \pm 12.07%, carnosine-treated group: 67.36 \pm 4.57%, $P = .012$; Figure 5).

Carnosine Decreased the mRNA and Protein Expression Level of ClpP in Cultured HeLa Cells

ClpP is related to the enzyme activity of complex II. In the current study, we also detected the mRNA and protein expression levels of ClpP and ClpX under the influence of carnosine in HeLa and SiHa cells. The result in Figure 6 showed that the mRNA and protein expressions of ClpP were both downregulated in HeLa cells after carnosine treatment, which is corresponding with complex II. However, the protein expression level of ClpX, which is the chaperone of ClpP, was not markedly changed.

Carnosine Retarded Cell Cycle and Reduced the Expression of c-Myc and PCNA Proteins in HeLa and SiHa Cells

In the current study, we also explored the role of carnosine in cell cycle progression in the cultured HeLa and SiHa cells. The data showed that carnosine treatment significantly

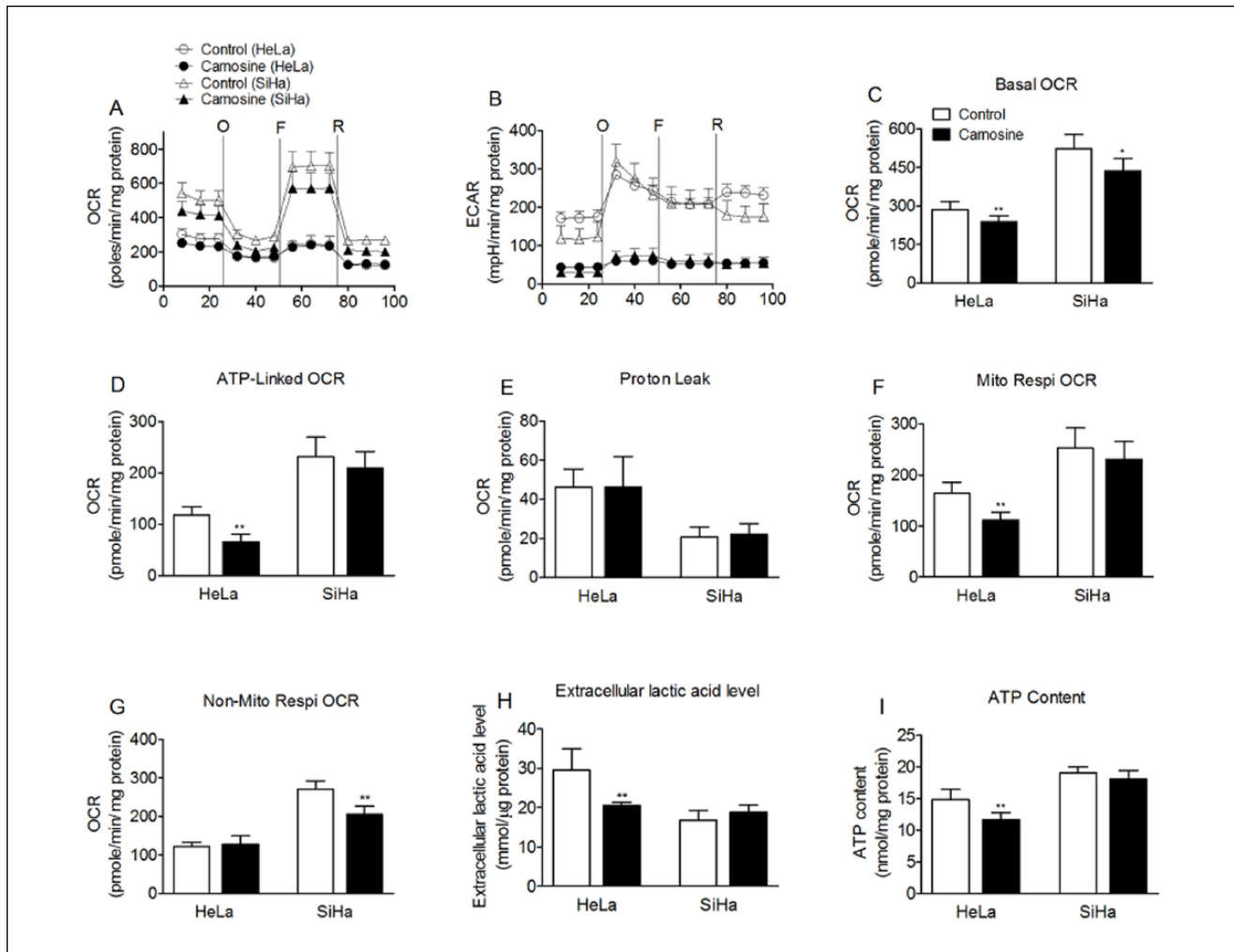


Figure 3. Effects of carnosine on mitochondrial respiration and glycolysis in cultured HeLa and SiHa cells. Real-time analysis of oxygen consumption rates (OCR) (A) and extracellular acidification rates (ECAR) (B) of cultured HeLa and SiHa cells by perturbing them with small molecule metabolic modulators. Oligomycin (O, 1 μ M), FCCP (F, 1 μ M), and rotenone (R, 1 μ M) were injected sequentially at the indicated time points into each well containing HeLa and SiHa cells after baseline rate measurement. (C) Basal OCR, (D) ATP-linked OCR, (E) proton leak, (F) mitochondrial respiration OCR, (G) non-mitochondrial respiration OCR, (H) extracellular lactic acid level, and (I) ATP content are shown. Each data represents mean \pm SD. N = 6-8. * P < .05, ** P < .01 versus control group.

increased the amount of cells in G1 phase (control group: $56.74 \pm 0.28\%$, carnosine-treated group: $63.86 \pm 1.61\%$, $P = .002$) and decreased the amount of cells in S phase (control group: $38.78 \pm 1.17\%$, carnosine-treated group: $28.51 \pm 0.12\%$, $P = .000$) in cultured HeLa cells (Figure 7A, B). We also found that carnosine caused a slight increase in the amount of cells in G1 phase (control group: $58.58 \pm 4.97\%$, carnosine-treated group: $63.04 \pm 3.95\%$, $P = .291$); however, it significantly decreased the amount of cells in S phase in cultured SiHa cells (control group: $23.55 \pm 1.30\%$, carnosine-treated group: $18.71 \pm 0.97\%$, $P = .007$; Figure 7A, C). Thus, all the data indicate that carnosine induces G1 arrest in HeLa and SiHa cells by inhibiting the G1-S phase transition. Next we measured the proteins expression level of proliferating cell nuclear antigen (PCNA; high-expressed in S

phase) and c-Myc, which promotes cell immortalization. The results showed that carnosine treatment significantly reduced the expression levels of PCNA and c-Myc both in the cultured HeLa and SiHa cells (Figure 7D).

The mRNA Expression Level of *PepT1* and *PepT2* in Cultured HeLa and SiHa Cells

In the current study, we found that the inhibitory effect of carnosine on the proliferative capacity in cultured HeLa cells is more effective than that in SiHa cells. We wondered whether this phenomenon is due to the different expression levels of *pepT1* and *pepT2*, the peptide transporters responsible for the transport of carnosine into the cells, in HeLa and SiHa cells. So we also examined the mRNAs expression

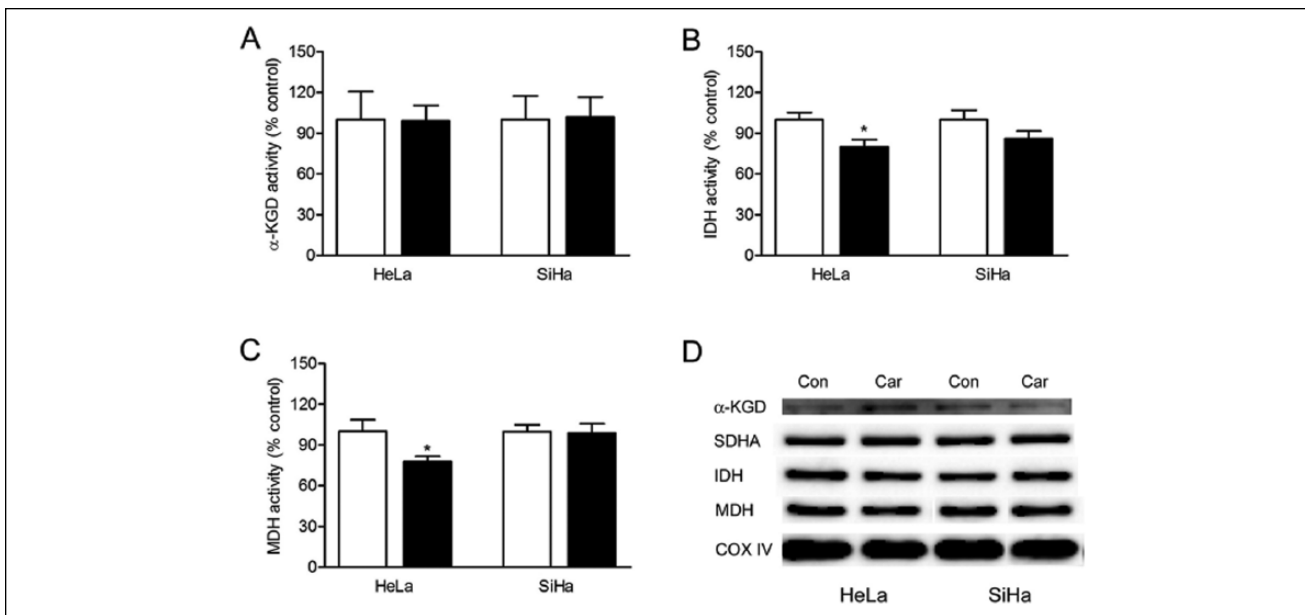


Figure 4. Effects of carnosine on the activity and expression level of dehydrogenases in the TCA in cultured HeLa and SiHa cells. The cells were treated with 20 mM carnosine for 48 hours, and then the enzyme activity of α -KGD (A), IDH (B), and MDH (C) was measured by spectrophotometry. Results were expressed as percentage of control, and were expressed as mean \pm SD. N = 3. * P < .05 versus control group. Western blot analysis of the expression of α -KGD, SDHA, IDH, and MDH in the mitochondria in cultured HeLa and SiHa cells (D).

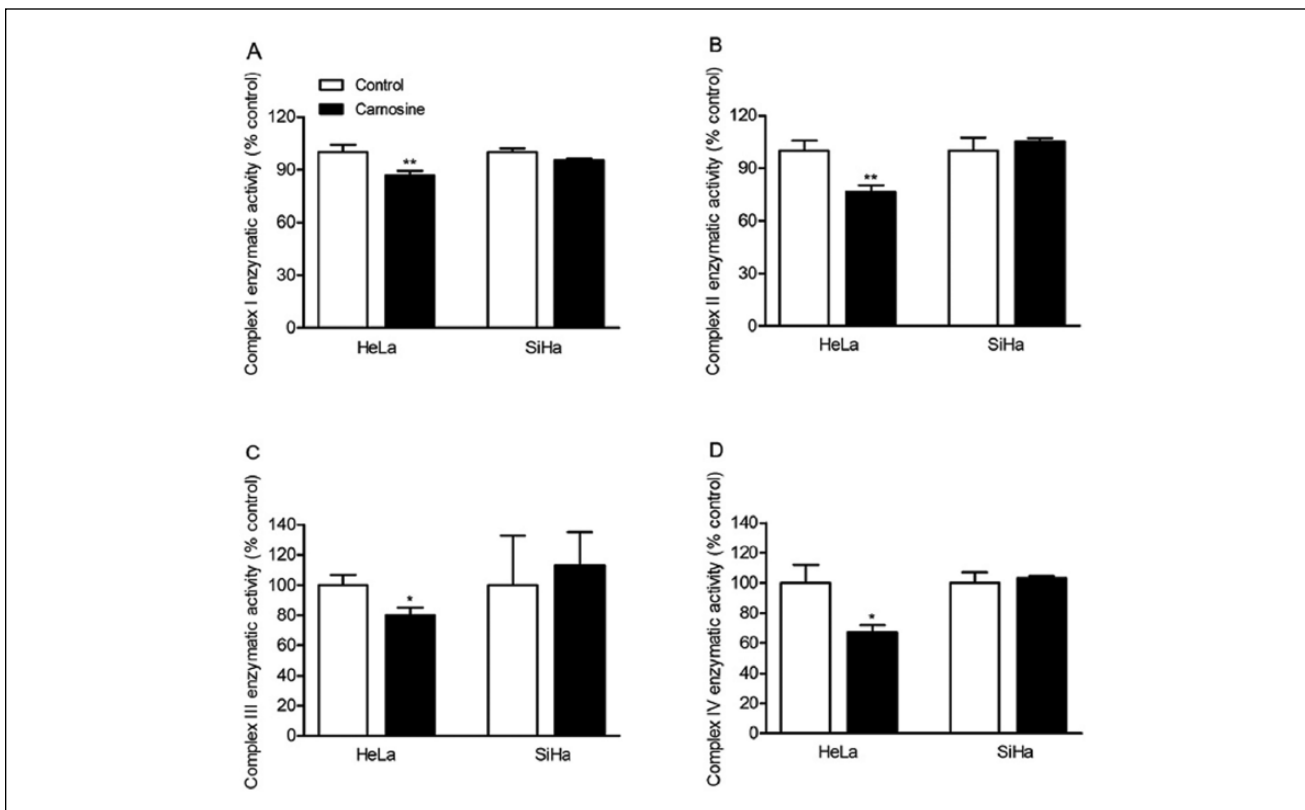


Figure 5. Effect of carnosine on the activity of mitochondrial ETC complexes in cultured HeLa and SiHa cells. The cells were treated with 20 mM carnosine for 48 hours, and then the activity of ETC complex I (A), complex II (B), complex III (C), and complex IV (D) was measured by spectrophotometry. Results were expressed as percentage of control, and were showed as mean \pm SD. N = 3-4. * P < .05, ** P < .01 versus control group.

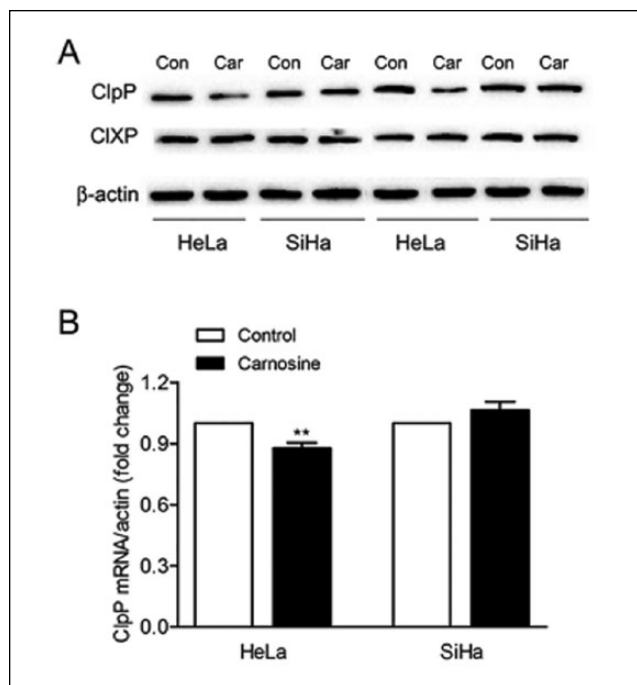


Figure 6. Effects of carnosine on the expression level of ClpP and ClpX in cultured HeLa and SiHa cells. The cells were treated with 20 mM carnosine for 48 hours, and the proteins expression levels of ClpP and ClpX were determined by western blot (A). Real-time PCR analysis of the mRNA expression level of ClpP in cultured HeLa and SiHa cells (B). Results were expressed as mean \pm SD. N = 3. ** $P < .01$ versus control group.

level of pepT1 and pepT2 in these 2 cell lines. We found that the mRNA expression level for pepT1 could be detected neither in HeLa nor in SiHa cells. However, the mRNA expression level for pepT2 in SiHa cells was much higher than that in HeLa cells (Figure 8).

Discussion

To our knowledge, this is the first study to evaluate the effects of carnosine on mitochondrial bioenergetics and cell proliferation in cultured human cervical carcinoma cells HeLa and SiHa. Our principal findings are as follows. First, carnosine significantly decreased the mitochondrial bioenergetics, glycolysis, and the proliferative capacity of HeLa cells but not SiHa cells. Second, carnosine markedly decreased the activities of IDH and MDH in TCA cycle and the ETC complexes I to IV in HeLa cells. Third, carnosine may decrease the activities of ETC complexes I and II in HeLa cells by downregulation of ClpP. Thus, carnosine may decrease the proliferation of HeLa cells by a selective inhibition of their mitochondrial metabolism.

Carnosine shows an inhibitory effect on the growth of transformed cells both in vitro and in vivo.²⁵ In the current

study, we observed a significant decrease in cell proliferative capacity of HeLa cells but not SiHa cells, and this effect was not accompanied by apoptosis. It has been demonstrated that carnosine may through suppressing glycolysis inhibit growth and proliferation of cancer cells.^{8,26} Here, we also found that carnosine treatment markedly suppressed glycolysis in cultured HeLa cells, and the results are consistent with the previous studies.²⁵ However, we do not know why carnosine treatment did not affect glycolysis in cultured SiHa cells.

Recently, mitochondrial function was found to play an important role in tumorigenesis, development, and metastasis of multiple cancer cell types.^{15,16,27} Thus, mitochondria have been considered as a novel and effective therapeutic target for treatment in some types of cancer. Our previous study found that carnosine also possesses a novel role as a regulator of mitochondrial respiration in cultured human gastric cancer SGC-7901 cells.¹⁸ In the current study, the Seahorse analysis showed that carnosine decreased the basal cellular OCR both in the HeLa and SiHa cells. This decrease was mainly due to the decreased mitochondrial respiration (ATP-linked respiration) in HeLa cells, whereas the decreased basal cellular OCR was mainly due to the decreased non-mitochondrial respiration (cytosolic oxygen consumption) in SiHa cells, indicating that the mitochondrial ATP output decreases in the carnosine-treated HeLa cells but not SiHa cells. Thus, carnosine may inhibit the proliferation of HeLa cells mainly by a suppression of glycolysis and mitochondrial bioenergetics. But the question remained of how carnosine regulates the mitochondrial bioenergetics.

The TCA cycle is a central metabolic pathway responsible for supplying reducing potential for oxidative phosphorylation and anabolic substrates for cell growth, repair, and proliferation, and inactivation of any step can disrupt mitochondrial bioenergetics.²⁸ In the current study, lower activities of IDH₃, MDH (Figure 4B, C) and SDH (assayed as mitochondrial ETC complex II activity; Figure 5B) were observed in cultured HeLa cells under the influence of carnosine. Similarly, it was shown that the MDH activity has fairly good correlation with the growth rate of tumors. The slow-growing tumors revealed less MDH activity compared with fast growing tumors.²⁹ However, recently Macedo et al showed that acute carnosine treatment enhanced cerebral cortex SDH activity, but it did not induce any change in MDH activity in rats.³⁰ This difference between HeLa cells and cerebral cortex tissue in response to carnosine may be due to the different energy metabolism of the transformed and non-transformed cells.

In this study, we also explored the role of ETC complexes I, II, III, and IV as potential pharmacological targets of carnosine in cultured HeLa and SiHa cells. We observed a statistically significant decrease of complexes I, II, III, and IV activities in HeLa cells but not in SiHa cells

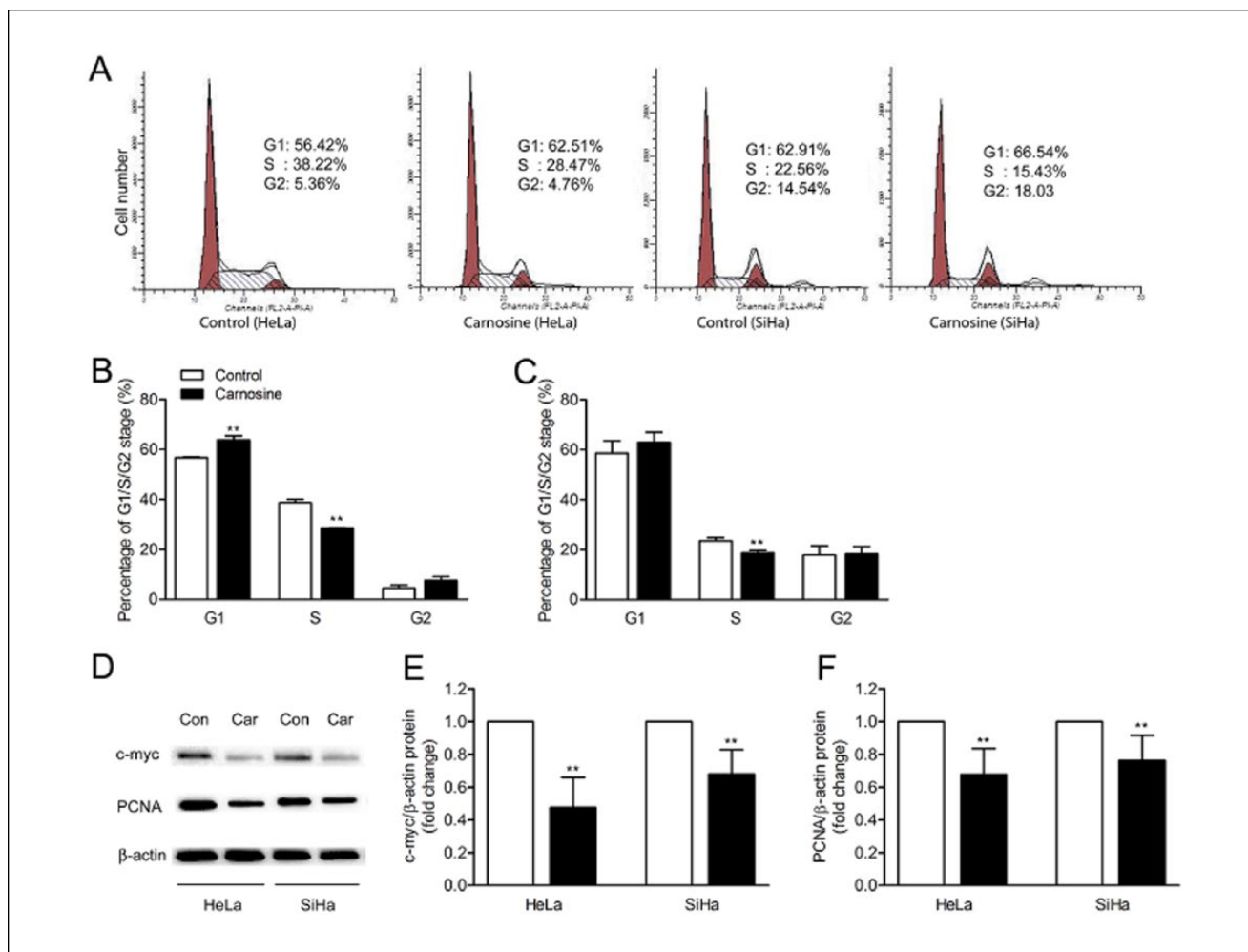


Figure 7. Carnosine inhibited cell cycle progression in cultured HeLa and SiHa cells. The HeLa and SiHa cells were treated with carnosine (20 mM) for 48 hours, and then the cell cycle distribution was measured by flow cytometry. Representative images of cell cycle progression analysis in cultured HeLa and SiHa cells (A). Statistical analysis of percentage of cells in each cell cycle phase in cultured HeLa cells (B) and SiHa cells (C). Western blot analysis of the expression level of c-Myc and PCNA in HeLa and SiHa cells after carnosine treatment for 48 hours (D). Densitometric analysis of bands for relative c-Myc (E) and PCNA (F) protein expression level. Data were shown as mean ± SD. **P < .01 versus control group.

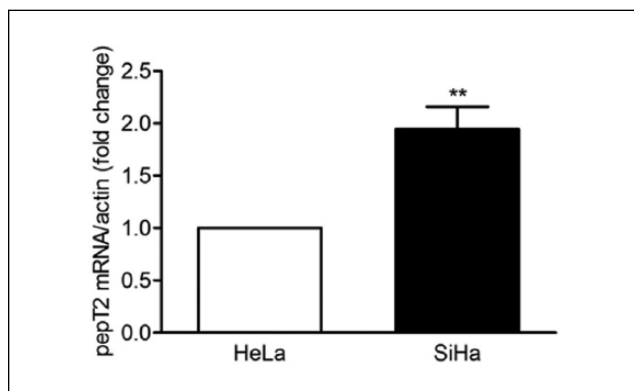


Figure 8. Real-time PCR analysis of the mRNA expression for pepT2 in cultured HeLa and SiHa cells. Results were expressed as mean ± SD. N = 3. **P < .01 versus HeLa cells.

receiving carnosine treatment for 48 hours. A literature report showed that rats receiving carnosine acutely presented reduced activity of complexes I-III and II, as well as a trend of decrease in complexes II and III activities in skeletal muscle.³¹ However, in cerebral cortex tissue of rats, acute carnosine treatment enhanced the activities of complexes I-III and II-III.³⁰ It has been shown that in the yeast *Saccharomyces cerevisiae*, carnosine produced contrasting effects on growth and viability, which suggested to be related to the organism's energy metabolism.³² Overall, these data indicate that carnosine can induce contrasting effects on the activities of the ETC complexes due to the different energy metabolism of the cells. Thus, the ETC complexes may be the potential pharmacological targets of carnosine. However, the molecular mechanisms behind this action of carnosine are still under investigation.

The ETC complexes I, II, and IV are coupled to H⁺ pumping from the matrix to intermembrane space to create the electrochemical gradient during the process of electron transfer. Thus, it is possible that carnosine suppresses the activities of the ETC complexes I, III, and IV because of its H⁺ buffering capacity, impairing the electrochemical gradient which is for complex V to generate ATP in HeLa cells.

ClpP is one of the primary quality control proteases in the mitochondrial matrix. Recently, ClpP has been observed to maintain mitochondrial protein homeostasis and is involved in regulating the activities of ETC complexes I and II and mitochondrial respiration.³³ In the current study, we found that carnosine treatment significantly reduced ClpP expression both at the transcription and translation levels in HeLa cells but not in SiHa cells. However, there was no significant difference observed in ClpX expression under the influence of carnosine in cultured HeLa and SiHa cells. Recently, it has been reported that reducing the levels of mitochondrial ClpP or ClpX renders human cancer cells more sensitive to cisplatin, a widely used anticancer drug.³⁴ Thus, we speculated that carnosine may inhibit the activities of complex I and complex II in HeLa cells by reducing ClpP expression. Therefore, ClpP may be a potential target for carnosine in cancer treatment.

On the other hand, carnosine has been reported to act as a regulator of cell cycle that plays a key role in regulating cell proliferation.^{11,35,36} Iovine et al reported that carnosine induces G1 arrest in human HCT116 colon cancer cells by inhibiting the G1/S phase transition.¹⁰ Our findings from flow cytometric analysis also showed that carnosine could suppress the transformation from G1 phase to S phase in cultured HeLa and SiHa cells. In addition, western blot analysis also demonstrated that carnosine reduced the expression levels of c-Myc, which plays a crucial role in cell growth and proliferation,³⁶ and PCNA, which is not expressed in resting cells but in proliferating cells,³⁷ both in cultured HeLa and SiHa cells. Thus, inhibition of proliferation of HeLa and SiHa cells by carnosine may be at least partly due to its action on cell cycle and its associated proteins.

However, at present, we do not know why the inhibitory action of carnosine on the proliferation in HeLa cells is more effective than that in SiHa cells. We speculated that it may be due to the different intracellular carnosine concentrations in HeLa and SiHa cells. However, the data showed that the mRNA level for pepT2 in SiHa cells was much higher than that in HeLa cells, indicating that the intracellular carnosine concentration in SiHa cells should not be lower than that in HeLa cells. It is currently not known whether the inhibitory effect of carnosine is mediated by one of its components, L-histidine or β -alanine, and whether the hydrolysis of the dipeptide is a prerequisite for its anti-neoplastic effect. Although there are hints from the literature that L-histidine can mimic the effect of carnosine,³⁸ it is

not known whether hydrolysis of carnosine is required nor do we know whether carnosine degrading enzymes are active in HeLa and SiHa cells. We are aware that more experiments need to be performed in the future to address these interesting questions in order to delineate the molecular mechanisms responsible for the bioactivity of carnosine on human cervical gland carcinoma cells and cervical squamous carcinoma cells.

Conclusions

Carnosine could significantly inhibit the proliferation of cultured human cervical gland carcinoma cells HeLa rather than cervical squamous carcinoma cells SiHa. Mitochondrial bioenergetics, glycolysis pathway, and cell cycle may be involved in the carnosine action on cell proliferation in cultured human cervical gland carcinoma cells HeLa.

Declaration of Conflicting Interests

The author(s) declared no potential conflicts of interest with respect to the research, authorship, and/or publication of this article.

Funding

The author(s) disclosed receipt of the following financial support for the research, authorship, and/or publication of this article: This work was supported by the National Natural Science Foundation of China (81571289).

References

1. Marx JL. Human papilloma virus and cervical cancer. *Science*. 1986;231:920.
2. Tzenov YR, Andrews PG, Voisey K, et al. Human papilloma virus (HPV) E7-mediated attenuation of retinoblastoma (Rb) induces hPygopus2 expression via Elf-1 in cervical cancer. *Mol Cancer Res*. 2013;11:19-30.
3. Bansal M, Li Z, Zhao C. Correlation of histopathologic/cytologic follow-up findings with vaginal ASC-US and ASC-H Papanicolaou test and HPV test results. *Am J Clin Pathol*. 2012;137:437-443.
4. Fiander AN. The prevention of cervical cancer in Africa. *Womens Health (Lond Engl)*. 2011;7:121-132.
5. Son DO, Satsu H, Kiso Y, Totsuka M, Shimizu M. Inhibitory effect of carnosine on interleukin-8 production in intestinal epithelial cells through translational regulation. *Cytokine*. 2008;42:265-276.
6. Fontana M, Pinnen F, Lucente G, Pecci L. Prevention of peroxynitrite-dependent damage by carnosine and related sulphonamido pseudodipeptides. *Cell Mol Life Sci*. 2002;59:546-551.
7. Nadi NS, Hirsch JD, Margolis FL. Laminar distribution of putative neurotransmitter amino acids and ligand binding sites in the dog olfactory bulb. *J Neurochem*. 1980;34:138-146.
8. Gaunitz F, Hipkiss AR. Carnosine and cancer: a perspective. *Amino Acids*. 2012;43:135-142.

9. Gallant S, Semyonova M, Yuneva M. Carnosine as a potential anti-senescence drug. *Biochemistry (Mosc)*. 2000;65:866-868.
10. Iovine B, Iannella ML, Nocella F, Pricolo MR, Bevilacqua MA. Carnosine inhibits KRAS-mediated HCT116 proliferation by affecting ATP and ROS production. *Cancer Lett*. 2012;315:122-128.
11. Jia H, Qi X, Fang S, et al. Carnosine inhibits high glucose-induced mesangial cell proliferation through mediating cell cycle progression. *Regul Pept*. 2009;154:69-76.
12. Renner C, Zemitzsch N, Fuchs B, et al. Carnosine retards tumor growth in vivo in an NIH3T3-HER2/neu mouse model. *Mol Cancer*. 2010;9:2.
13. Horii Y, Shen J, Fujisaki Y, Yoshida K, Nagai K. Effects of L-carnosine on splenic sympathetic nerve activity and tumor proliferation. *Neurosci Lett*. 2012;510:1-5.
14. Sale C, Artioli GG, Gualano B, Saunders B, Hobson RM, Harris RC. Carnosine: from exercise performance to health. *Amino Acids*. 2013;44:1477-1491.
15. Diers AR, Broniowska KA, Chang CF, Hogg N. Pyruvate fuels mitochondrial respiration and proliferation of breast cancer cells: effect of monocarboxylate transporter inhibition. *Biochem J*. 2012;444:561-571.
16. Barbi de Moura M, Vincent G, Fayewicz SL, et al. Mitochondrial respiration: an important therapeutic target in melanoma. *PLoS One*. 2012;7:e40690.
17. Spinazzi M, Casarin A, Pertegato V, Salviati L, Angelini C. Assessment of mitochondrial respiratory chain enzymatic activities on tissues and cultured cells. *Nat Protoc*. 2012;7:1235-1246.
18. Shen Y, Yang J, Li J, et al. Carnosine inhibits the proliferation of human gastric cancer SGC-7901 cells through both of the mitochondrial respiration and glycolysis pathways. *PLoS One*. 2014;9:e104632.
19. Shen Y, Tian Y, Yang J, et al. Dual effects of carnosine on energy metabolism of cultured cortical astrocytes under normal and ischemic conditions. *Regul Pept*. 2014;192-193:45-52.
20. Shi L, Wang Y, Tu S, et al. The responses of mitochondrial proteome in rat liver to the consumption of moderate ethanol: the possible roles of aldo-keto reductases. *J Proteome Res*. 2008;7:3137-3145.
21. Humphries KM, Szweda LI. Selective inactivation of alpha-ketoglutarate dehydrogenase and pyruvate dehydrogenase: reaction of lipoic acid with 4-hydroxy-2-nonenal. *Biochemistry*. 1998;37:15835-15841.
22. Liu TF, Vachharajani V, Millet P, Bharadwaj MS, Molina AJ, McCall CE. Sequential actions of SIRT1-RELB-SIRT3 coordinate nuclear-mitochondrial communication during immunometabolic adaptation to acute inflammation and sepsis. *J Biol Chem*. 2014;290:396-408.
23. Schmittgen TD, Livak KJ. Analyzing real-time PCR data by the comparative C(T) method. *Nat Protoc*. 2008;3:1101-1108.
24. Nolan T, Hands RE, Bustin SA. Quantification of mRNA using real-time RT-PCR. *Nat Protoc*. 2006;1:1559-1582.
25. Holliday R, McFarland GA. Inhibition of the growth of transformed and neoplastic cells by the dipeptide carnosine. *Br J Cancer*. 1996;73:966-971.
26. Hipkiss AR, Gaunitz F. Inhibition of tumour cell growth by carnosine: some possible mechanisms. *Amino Acids*. 2014;46:327-337.
27. LeBleu VS, O'Connell JT, Gonzalez Herrera KN, et al. PGC-1alpha mediates mitochondrial biogenesis and oxidative phosphorylation in cancer cells to promote metastasis. *Nat Cell Biol*. 2014;16:992-1003, 1001-1015.
28. Bubber P, Hartounian V, Gibson GE, Blass JP. Abnormalities in the tricarboxylic acid (TCA) cycle in the brains of schizophrenia patients. *Eur Neuropsychopharmacol*. 2011;21:254-260.
29. Bhatt DK, Bano M. Modulation of tricarboxylic acid cycle dehydrogenases during hepatocarcinogenesis induced by hexachlorocyclohexane in mice. *Exp Toxicol Pathol*. 2009;61:325-332.
30. Macedo LW, Cararo JH, Maravai SG, et al. Acute carnosine administration increases respiratory chain complexes and citric acid cycle enzyme activities in cerebral cortex of young rats. *Mol Neurobiol*. 2016;53:5582-5590.
31. Macarini JR, Maravai SG, Cararo JH, et al. Impairment of electron transfer chain induced by acute carnosine administration in skeletal muscle of young rats. *Biomed Res Int*. 2014;2014:632986.
32. Cartwright SP, Bill RM, Hipkiss AR. L-carnosine affects the growth of *Saccharomyces cerevisiae* in a metabolism-dependent manner. *PLoS One*. 2012;7:e45006.
33. Deepa SS, Bhaskaran S, Ranjit R, et al. Down-regulation of the mitochondrial matrix peptidase ClpP in muscle cells causes mitochondrial dysfunction and decreases cell proliferation. *Free Radic Biol Med*. 2015;91:281-292.
34. Zhang Y, Maurizi MR. Mitochondrial ClpP activity is required for cisplatin resistance in human cells. *Biochim Biophys Acta*. 2016;1862:252-264.
35. Zhang Z, Miao L, Wu X, et al. Carnosine inhibits the proliferation of human gastric carcinoma cells by retarding Akt/mTOR/p70S6K signaling. *J Cancer*. 2014;5:382-389.
36. Schuhmacher M, Eick D. Dose-dependent regulation of target gene expression and cell proliferation by c-Myc levels. *Transcription*. 2013;4:192-197.
37. Sasaki K, Kurose A, Ishida Y. Flow cytometric analysis of the expression of PCNA during the cell cycle in HeLa cells and effects of the inhibition of DNA synthesis on it. *Cytometry*. 1993;14:876-882.
38. Letzien U, Oppermann H, Meixensberger J, Gaunitz F. The antineoplastic effect of carnosine is accompanied by induction of PDK4 and can be mimicked by L-histidine. *Amino Acids*. 2014;46:1009-1019.